

Layer Attitude and Thickness Measurements of the three Interior Layered Deposits Mounds within Juventae Chasma, Mars. N. Novakovic¹, F. Fueten¹, J. Flahaut², R. Stesky³, A.P. Rossi⁴, E. Hauber⁵, ¹Department of Earth Sciences, Brock University, St. Catharines, Ontario, Canada L2S 3A1 <ffueten@brocku.ca>; ²Vrije Universiteit Amsterdam (VU), The Netherlands; ³Pangaea Scientific, Brockville, Ontario, Canada K6V 5T5; ⁴Jacobs University Bremen, 28759 Bremen, Germany; ⁵Institute of Planetary Research, German Aerospace Center (DLR), Berlin, Germany

Introduction: Formation of the chasmata of Valles Marineris (Fig 1A) is thought to have taken place during a two-stage process [1, 2]. Early ancestral basin formation was followed by the linking of the basins into their current geometry [3, 1]. Interior layered deposits (ILDs) occur throughout the chasmata of Valles Marineris [1] and are diverse in thickness, albedo, mineral compositions, and erosional characteristics. Multiple infill mechanisms have been proposed (see references in [4]). ILDs are associated with hydrated minerals, which are linked with water and can thus provide valuable information on the early history of Mars (see references in [5, 6])

Examination of the layering can help to narrow the range of deposition mechanisms [e.g 4]. Here we measure layer attitudes and thicknesses within three ILD mounds (Fig. 1B, white A, B, C) within Juventae Chasma which have previously been mapped [7].

Juventae Chasma: Juventae Chasma (Fig. 1A) is a ~5 km deep chasm, 500 km to the north of Valles Marineris [7]. The chasm is believed to have once held large quantities of water which would have flowed out of the chasma through a large outflow channel located on its northern end, Maja Vallis [7]. Within the chasm, interior layered deposits (ILDs) outcrop at four different locations, and are named from south to north mound A to D [7]. Data from seven HiRISE images [Table 1] were used to determine the layer thickness and geometry of three of these mounds.

Methodology: A CTX mosaic was map projected in ISIS (Fig 1B) and seven HiRISE stereo images and DTMs were calculated using the NASA Ames Stereo pipeline [8, 9] and rescaled to 1m/pixel. Layer geometry was determined by measuring the strike and dip of layers using the ORION software package and further analyzed using SpheriStat 3.2 software. Individual layer thicknesses were measured in the GIS software Global Mapper. Points were placed along individual layer boundaries within a layer package to determine elevations.

Results: Layer thicknesses for mounds A and C are similar with an average layer thicknesses of 2.6 m and 3.2 m respectively (Fig. 1C). Layer thickness for mound B is significantly different, with an average layer thickness of 83.5 m (Fig. 1D).

Layer attitudes are generally shallow (Fig. 1B see stereonets). At the northern portion of mound C, the lowest visible layering mimics adjacent basement topography (Fig. 1E). The dip of the layering in mound B is nearly sub-horizontal and becomes shallower with increasing elevation.

Visual Observations: Distinct packages of deformed layers exhibiting slump features and truncations exist between packages of non-deformed layers on mound C (Fig. 1F).

No internal structures are visible within the thicker layer packages on Mound B. Oblique grooves, which cross multiple layers, are clearly erosional features (Fig. 1G).

Discussion: The basal layers at mound C clearly indicate that ILD deposition post-dates basement topography. Packages affected by soft-sedimentary deformation may indicate episodic disruption (tectonic or impact-related) throughout the deposition history. The depositional mechanisms for mounds A and C are potentially different from those of Mound B.

Analysis of CRISM data is currently in progress. This work is part of a project with the aim to document stratigraphic relationships and compare layer thicknesses with other ILDs within Valles Marineris.

References: [1] Lucchitta, B.K. et. al., (1994), *J. Geophys. Res.*, 99, 3783-3798. [2] Schultz, R. A. (1998), *Planet. Space Sci.*, 46, 827-829, doi:10.1016/S0032-0633(98)00030-0. [3] Lucchitta, B. K., and M. L. Bertolini (1990), *Lunar Planet. Sci.*, XX, 590-591. [4] Fueten, F. et al. (2010), *EPSL*, 294, 343-356, doi:10.1016/j.epsl.2009.11.004. [5] Flahaut, F. et al. (2010), *J. Geophys. Res.*, 115, E11007, doi:10.1029/2009JE003566. [6] Flahaut, F. et al. (2010), *Icarus* 207, 175-185, doi:10.1016/j.icarus.2009.11.019 [7] Catling et al., 2006, *Icarus*, 181, 26-51 [8] Moratto, Z.M., et al. (2010). LPS XLI, Abstract #2364. [9] Broxton, M.J. and Edwards, L.J. (2008). LPS XXXIX, Abstract #2419.

Table 1: HiRISE images used (corresponding stereo pairs not listed):

Mound A	Mound B	Mound C
ESP_017279_1755	ESP_020470_1755	PSP_007060_1760
PSP_004291_1755	PSP_002379_1755	PSP_006915_1760
		ESP_015934_1760

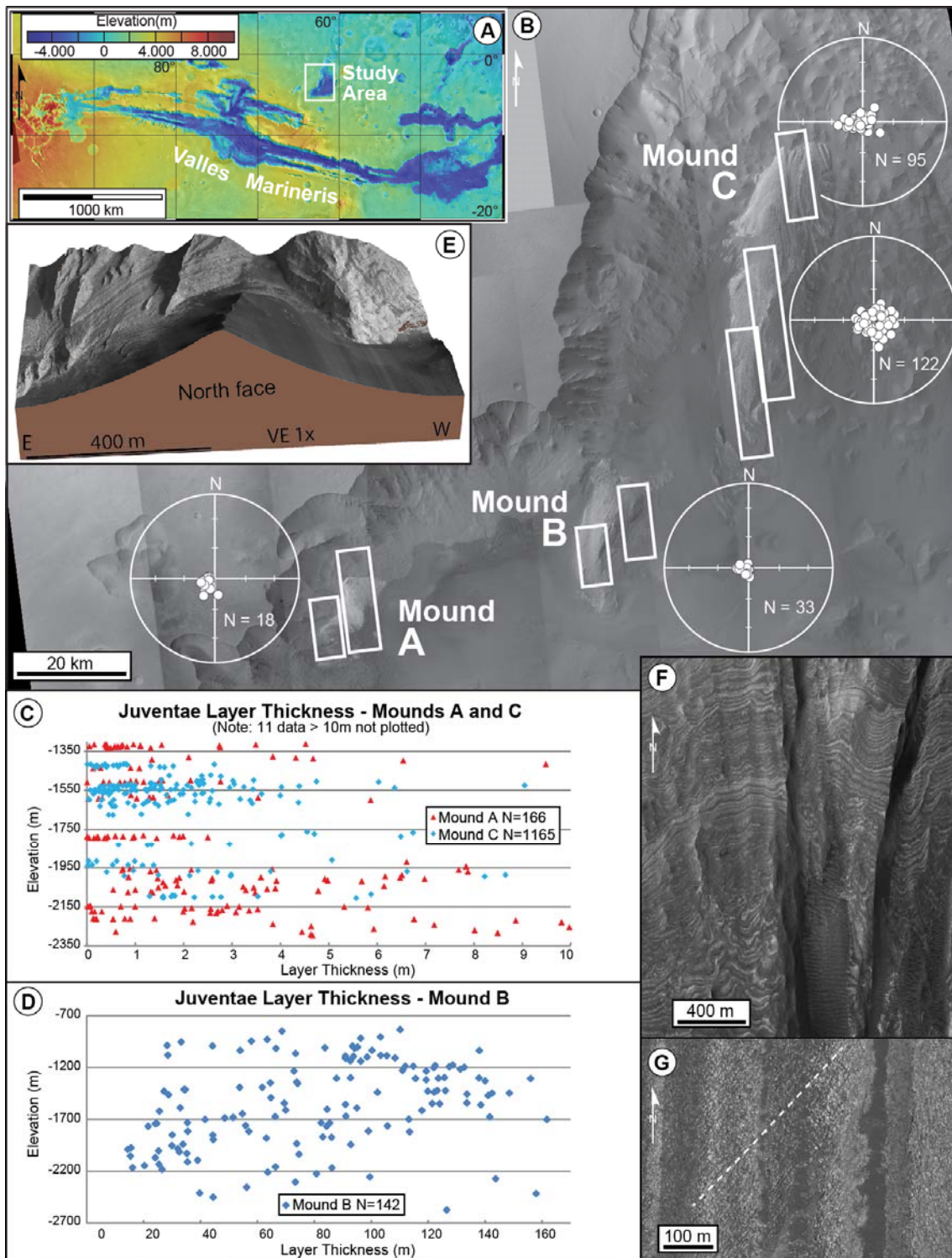


Figure 1: A) Location of study area. B) CTX Mosaic, locations of study sites, including stereonets of layer attitudes. C, D) Layer thickness vs. elevation; E) Deformed and unreformed layer packages near the base of mound C, F) layering in Mound B with surface grooves parallel to white dashed line.